CHEMISTRY
AN ASIAN JOURNAL

DOI: 10.1002/asia.201200186

# A Pentacyclic Nitrogen-Bridged Thienyl–Phenylene–Thienyl Arene for Donor–Acceptor Copolymers: Synthesis, Characterization, and Applications in Field-Effect Transistors and Polymer Solar Cells

**Cheng-An Tseng, Jhong-Sian Wu, Tai-Yen Lin, Wei-Shun Kao, Cheng-En Wu, So-Lin Hsu, Yun-Yu Liao, Chain-Shu Hsu, Huan-Yi Huang, You-Zung Hsieh, and Yen-Ju Cheng*[a]**

**Abstract:** A pentacyclic benzodipyrrolothiophene (**BDPT**) unit, in which two outer thiophene rings are covalently fastened with the central phenylene ring by nitrogen bridges, was synthesized. The two pyrrole units embedded in **BDPT** were constructed by using one-pot palladium-catalyzed amination. The coplanar stannylated Sn-BDPT building block was copolymerized with electron-deficient thieno[3,4-*c*]pyrrole-4,6-dione (**TPD**), benzothiadiazole (**BT**), and dithienyl-diketopyrrolopyrrole (**DPP**) acceptors by Stille polymerization. The bridging nitrogen atoms make the **BDPT** motif highly electron-abundant and structurally coplanar, which allows for tailoring the optical and electronic properties of the resultant polymers. Strong photoinduced charge-transfer with significant band-broadening in the solid state and relatively higher oxidation potential are characteristic of the BDPT-based polymers. Poly(benzodipyrrolothiophe*n*e-*alt*-benzothiadiazole) (**PBDPTBT**) achieved the highest field-effect hole mobility of up to $0.02\ cm^2\ V^{-1}\ s^{-1}$. The photovoltaic device using the **PBDPTBT**/$PC_{71}BM$ blend (1:3, w/w) exhibited a $V_{oc}$ of 0.6 V, a $J_{sc}$ of $10.34\ mA\ cm^{-2}$, and a FF of 50%, leading to a decent PCE of 3.08%. Encouragingly, the device incorporating poly(benzodipyrrolothiophene-*alt*-thienopyrrolodione) (**PBDPTTPD**)/$PC_{71}BM$ (1:3, w/w) composite delivered a highest PCE of 3.72%. The enhanced performance arises from the lower-lying HOMO value of **PBDPTTPD** to yield a higher $V_{oc}$ of 0.72 V.

**Keywords:** arenes · catalysis · copolymerization · field-effect transistors · solar cells

## Introduction

Polymer solar cells (PSCs) have attracted considerable interest because of their low-cost, light-weight, large-area, and flexible photovoltaic devices.[1] To achieve high efficiency of PSCs, the most critical challenge at the molecular level is to develop solution processable conjugated polymers that possess a low band-gap (LBG) to capture more solar photons and high hole mobility for efficient charge transport. The most effective method to develop a LBG polymer is to connect electron-rich donor and electron-deficient acceptor units along the conjugated polymer backbone.[2] On the basis of this molecular strategy, extensive research has been directed to developing new electron-rich donor segments for *p*-type materials. Forced planarization by covalently fastening adjacent aromatic units in a polymeric backbone can facilitate π-electron delocalization and elongate effective conjugation length, thus effectively reducing the optical band-gap.[3] Furthermore, chemical rigidification restricts the rotational disorder around interannular single bonds to reduce the reorganization energy, thus enhancing intrinsic charge mobility.[4] Consequently, multifused aromatic rings with forced planarity is a common structural feature of donor segments for recent successful LBG conjugated polymers. Thiophene and benzene aromatic rings are the most important structural ingredients to comprise photoactive *p*-type conjugated polymers. Integration of thiophene and benzene units into a rigid and coplanar entity has furnished a variety of fascinating ladder-type π-conjugated units.[5] For instance, the tricyclic benzodithiophene unit represents one of the most successful building blocks for making various low-band gap polymers that have made a breakthrough to achieve highly efficient polymer solar cells.[6] However, further elongation of mutually fused thiophene/benzene conjugated systems is synthetically challenging and it is inevitable to encounter solubility problems due to strong intermolecular aggregation. Another useful molecular design is to chemically coplanarize two adjacent thiophene/benzene units through a bridging element that allows for introducing solubilizing aliphatic side chains.[7] In this regard, carbon (C), silicon (Si), and nitrogen (N) are the most suitable bridging atoms

[a] C.-A. Tseng, J.-S. Wu, T.-Y. Lin, W.-S. Kao, C.-E. Wu, S.-L. Hsu, Y.-Y. Liao, Prof. Dr. C.-S. Hsu, H.-Y. Huang, Prof. Dr. Y.-Z. Hsieh, Prof. Dr. Y.-J. Cheng
Department of Applied Chemistry
National Chiao Tung University
1001 Ta Hsueh Road, Hsin-Chu, 30010 (Taiwan)
E-mail: yjcheng@mail.nctu.edu.tw

Supporting information for this article is available on the WWW under http://dx.doi.org/10.1002/asia.201200186.

to fasten two neighboring aryl rings, thereby forming five-membered cyclopentadiene, silole, and pyrrole rings, respectively, that are embedded in a multifused system.[7] Utilization of bridging elements featuring different steric and electronic properties will provide a useful tool to manipulate electronic and optical properties of the conjugated system. Pentacyclic indacenodithiophene (**IDT**) (Scheme 1) is a $C_{2h}$-symmetrical and coplanar unit with $sp^3$ carbon bridges to rigidify the central benzene ring and the two outer thiophene rings.[8] The **IDT**-based polymers have shown good charge-transporting properties leading to the high performance of solar cells and high field-effect mobilities.[9] Recently, Jen and co-workers reported the synthesis of a silicon-bridged analogue of the **IDT** unit, benzobis(silolothiophene) (**BST**), and the **BST**-based donor–acceptor polymer has also shown promise for photovoltaic applications.[10] It is highly desirable to chemically modify this thienyl–phenylene–thienyl system by employing a nitrogen element to substitute carbon bridges in **IDT** or silicon bridges in **BST**. As such, a new pentacyclic benzodipyrrolothiophene (**BDPT**) structure with two pyrrole units inserted between the thiophene and benzene units has been reported recently by Donaghey et al.[11] In parallel research, we report here a one-pot cyclization approach to successfully construct a **BDPT** structure by palladium-catalyzed amination of a key intermediate, 2,2′-(2,5-dibromo-1,4-phenylene)bis(3-bromothiophene). The N-bridged **BDPT** monomer was used as the electron-rich donor to copolymerize with the benzothiadiazole (**BT**), thieno[3,4-*c*]pyrrole-4,6-dione (**TPD**), and dithienyl-diketopyrrolopyrrole (**DPP**) acceptors, affording three alternating donor–acceptor copolymers poly(benzodipyrrolothiophe*ne*-*alt*-benzothiadiazole) (**PBDPTBT**), poly(benzodipyrrolothiophene-*alt*-thienopyrrolodione) (**PBDPTTPD**), and poly(benzodipyrrolothiophene-*alt*-dithienyldiketopyrrolopyrrole) (**PBDPTDPP**). Their thermal, optical, and electrochemical properties have been carefully characterized. The electronic and steric effect of the bridged-nitrogen on the molecular properties will be discussed in detail. These polymers have shown promise for applications in field-effect transistors and solar cell devices.

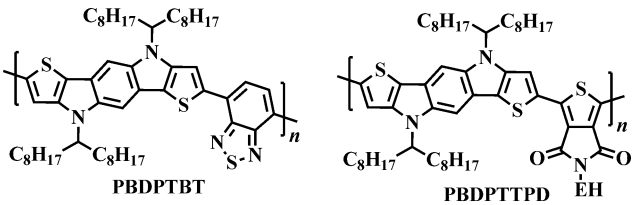


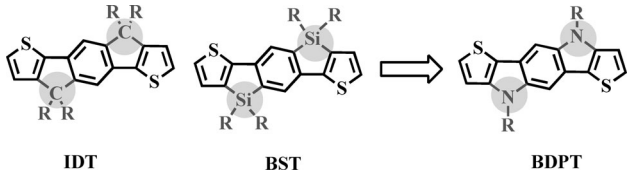


Scheme 1. Pentacyclic C-bridged **IDT**, Si-bridged **BST**, and N-bridged **BDPT** based on the thienyl–phenylene–thienyl structure.

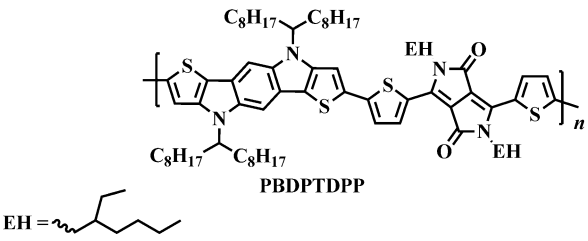


## Results and Discussion

### Synthesis

The synthetic procedure is shown in Scheme 2. Treatment of 2,3-dibromothiophene **1** with *n*-butyllithium followed by treatment with zinc bromide generated intermediate compound **2** that undergoes Negishi coupling with 1,4-dibromo-2,6-diiodobenzene **3** to afford 2,2′-(2,5-dibromo-1,4-phenylene)bis(3-bromothiophene) **4**. In the presence of $[Pd_2(dba)_3]$ (dba = dibenzylideneacetone) as the catalyst and 2,2'-bis(diphenylphosphino)-1,1'-binaphthyl (BINAP) as the ligand, **BDPT** was successfully synthesized by treating tetrabromo-intermediate **4** with 1-octylnonylamine by means of Buchwald–Hartwig amination. It should be noted that an excess amount of 1-octylnonylamine (11 equivalents) is required to successfully carry out intramolecular amination to form two pyrrole units in one pot. An attempt to carry out bromination at the 2,7-positions of the thiophene units was not suc-

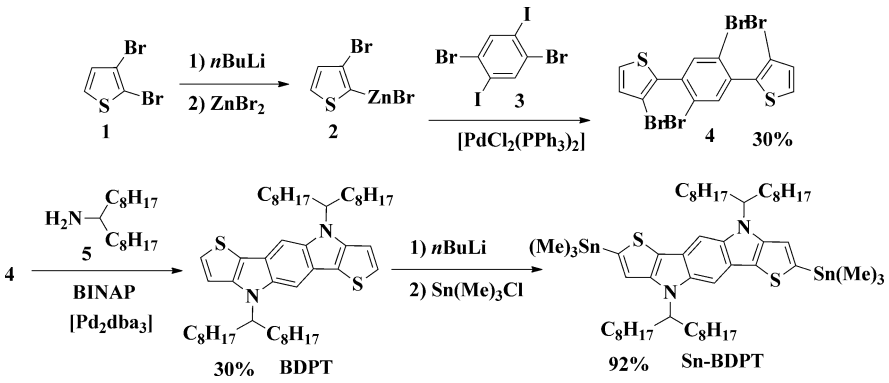


Scheme 2. Synthetic route for the **Sn-BDPT** monomer.

  

cessful due to the fact that the 5,10-positions at the central phenylene ring are also highly reactive as a result of the nitrogen-activation effect. Fortunately, the 2,7-positions of **BDPT** can be efficiently lithiated by *n*-butyllithium followed by reacting with trimethyltin chloride to afford **Sn-BDPT** in 92% yield. With the pentacylic **Sn-BDPT** monomer in hand, the copolymers **PBDPTBT**, **PBDPTTPP**, and **PBDPTDPP** were prepared by treating **Sn-BDPT** with **6**, **7**, and **8** monomers by using microwave-assisted Stille polymerization (Scheme 3). The molecular weights and PDI values

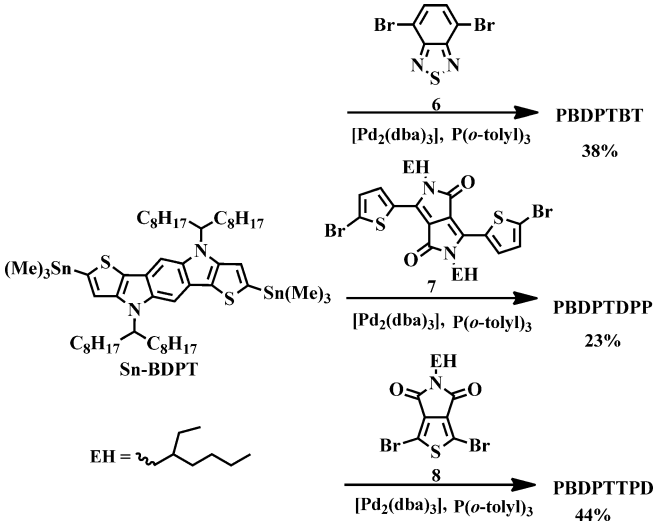


Scheme 3. Stille polymerization toward **PBDPTBT**, **PBDPTDPP**, and **PBDPTTPD**.

of the resultant polymers are shown in Table 1. All of the monomers and corresponding copolymers were fully characterized by NMR spectroscopy (see the Supporting Information). As a result of the branched 1-octylnonyl side chains used to promote solubility, the resulting copolymers showed excellent solubilities in common organic solvents, such as chloroform, toluene, chlorobenzene, and 1,2-dichlorobenzene.

### Thermal Properties

Thermal properties of the copolymers were analyzed by differential scanning calorimetry (DSC) and thermal gravimetric analysis (TGA) and summarized in Table 1. **PBDPTBT** and **PBDPTTPD** showed higher decomposition temperatures ($T_d$) at approximately 430 °C, whereas **PBDPTDPP** exhibited a lower $T_d$ at 395 °C (see Figure S1 in the Supporting Information), which demonstrated the sufficiently high thermal stability for PSCs applications. Based on the DSC analysis, **PBDPTBT** and **PBDPTTPD** are amorphous, whereas **PBDPTDPP** using **DPP** as the acceptor showed a crystalline nature with the observation of a melting point at 253 °C during heating and a crystallization point at 230 °C during cooling (Figure 1).

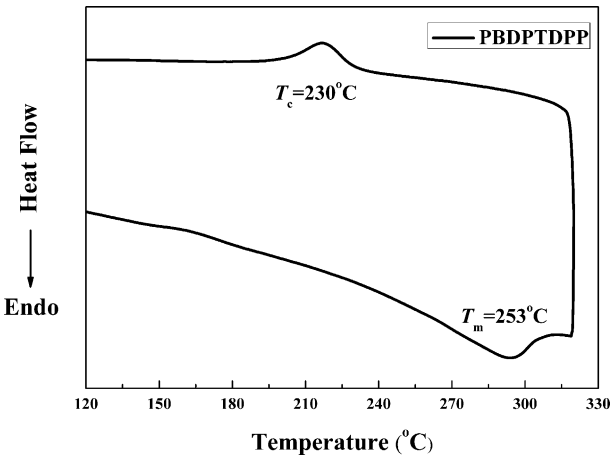


Figure 1. Differential scanning calorimetry (DSC) of **PBDPTDPP** at a heating rate of 10 °C min$^{-1}$.

### Optical Properties

All the N-bridged copolymers showed significant band-broadening and bathochromic-shift from the solution state to the solid state, which indicated that strong interchain π–π interactions take place due to the coplanar pentacyclic structures. It is noteworthy to mention that **PBDPTDPP** should have the highest degree of the intermolecular ordering in the solid state, considering that the full width at half maximum (FWHM) is dramatically increased from 128 nm in the solution state to 322 nm in the solid state, which is highly correlated with its crystalline nature. The optical band gaps ($E_g^{opt}$) deduced from the absorption edges of thin film spectra are in the following order: **PBDPTDPP** (1.25 eV) < **PBDPTBT** (1.52 eV) < **PBDPTTPD** (1.77 eV) (Figure 2), which means that the electron-accepting strength is in the order of: **DPP** > **BT** > **TPD**. Also note that the absorption edge of **PBDPTDPP** is located at a very low energy of approximately 1200 nm, which indicates that strong intramolecular charge transfer occurs from the highly electron-rich **BDPT** unit to the highly electron-deficient **DPP** unit and strong intermolecular interaction in the solid state. To gain more insight into the structure–property relationship, it is of importance to compare the optical properties of **PBDPTBT** with its

Table 1. Summary of the intrinsic properties of the **BDPT**-based polymers.

| Polymer | $M_n$ [kDa] | PDI | $T_g$ [°C] | $T_d$ [°C] | $T_m$ [°C] | $E_g^{opt}$ [eV] (Film) | $\lambda_{max}$ [nm] | | HOMO [eV] | LUMO [eV] |
|---|---|---|---|---|---|---|---|---|---|---|
| | | | | | | | toluene | film | | |
| **PBDPTBT** | 7.4 | 1.37 | 63 | 430 | – | 1.52 | 418, 691 | 431 731 | −5.11 | −3.25 |
| **PBDPTDPP** | 26.4 | 3.49 | 64 | 395 | 253 | 1.25 | 424, 745 | 431 829 | −4.89 | −3.41 |
| **PBDPTTPD** | 12.3 | 1.60 | 64 | 430 | – | 1.77 | 512, 584, | 516 605 | −5.14 | −3.13 |
| | | | 232 | | | | 630 | 656 | | |

  

CHEMISTRY
AN ASIAN JOURNAL

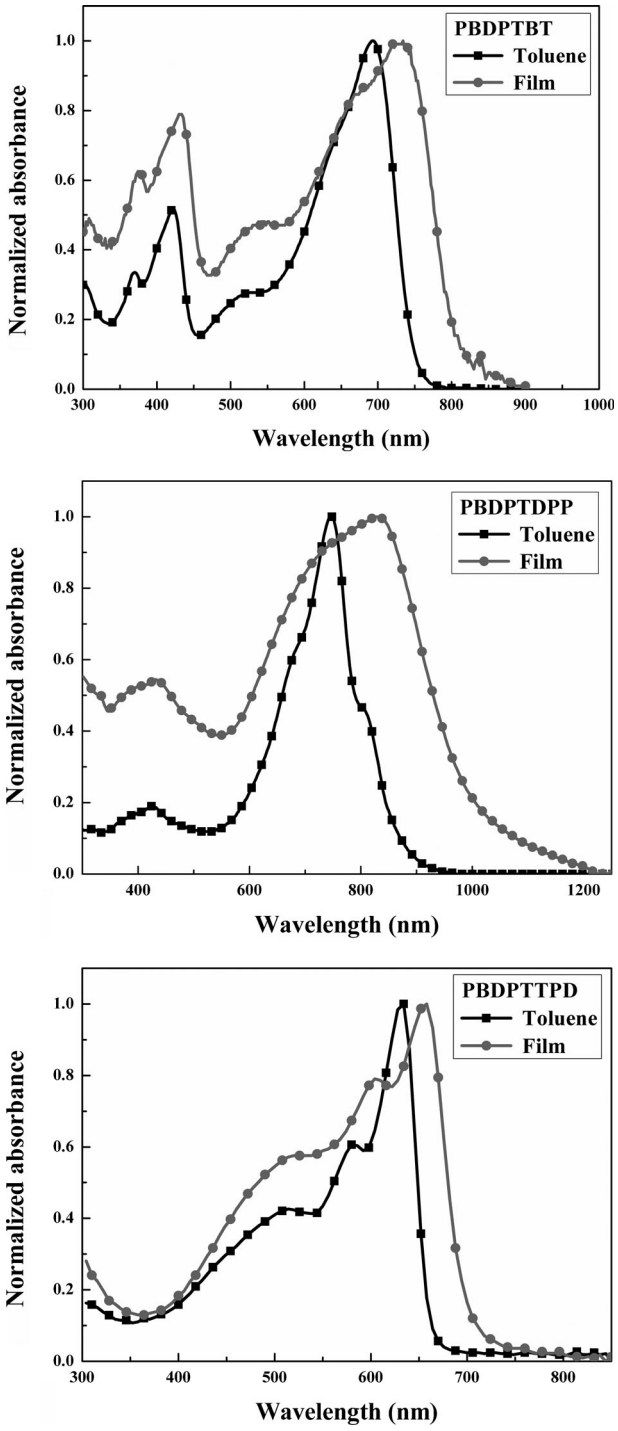


Figure 2. Normalized absorption spectra of **PBDPTBT** (top), **PBDPTDPP** (middle), and **PBDPTTPD** (bottom) in toluene solution and the solid state.

carbon-bridged poly(indacenodithiophene-*alt*-benzothiadiazole) **PIDTBT**[9] and silicon-bridged poly(benzobis(silolothiophene)-*alt*-benzothiadiazole) **PBSTTBT**[10] analogues with identical polymer composition except that the bridge atoms are different in the pentacyclic moieties. It is found that **PBDPTBT** exhibited a pronounced redshift absorption maximum wavelength $\lambda_{max}$ at 731 nm and smallest $E_g^{opt}$ of 1.52 eV, relative to **PBSTTBT** with a $\lambda_{max}$ at 636 nm and $E_g^{opt}$ of 1.8 eV, and **PIDTBT** with $\lambda_{max}$ at 630 nm and $E_g^{opt}$ of 1.75 eV.[9,10] Both the electronic and steric effects of the bridging atoms come into play in determining the optical behaviors. First, **BDPT** is the most electron-rich unit due to its nitrogen-donating ability, thereby inducing ICT with the lowest transition energy. Second, relative to the $sp^3$ hybridization of C and Si bridges consisting of two side chains sticking out of the conjugation plane, one branch aliphatic side chain on the nitrogen bridges in **BDPT** releases the steric hindrance near the backbone, which in turn promotes stronger intermolecular interactions.

## Electrochemical Properties

Cyclic voltammetry (CV) was used to evaluate the electrochemical properties and determine the HOMO and LUMO levels of the polymers (Table 1 and Figure 3). All of the polymers showed stable and reversible *p*-doping processes, which are prerequisites for semiconductor materials. The

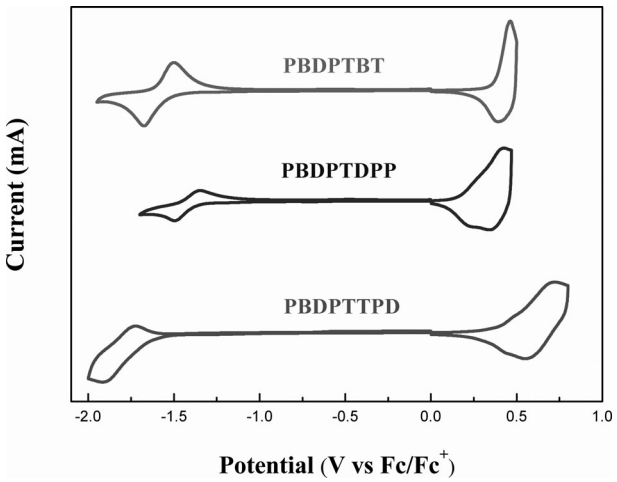


Figure 3. Cyclic voltammograms of **PBDPTBT**, **PBDPTDPP**, and **PBDPTTPD** in the thin film at a scan rate of 50 mV s$^{-1}$.

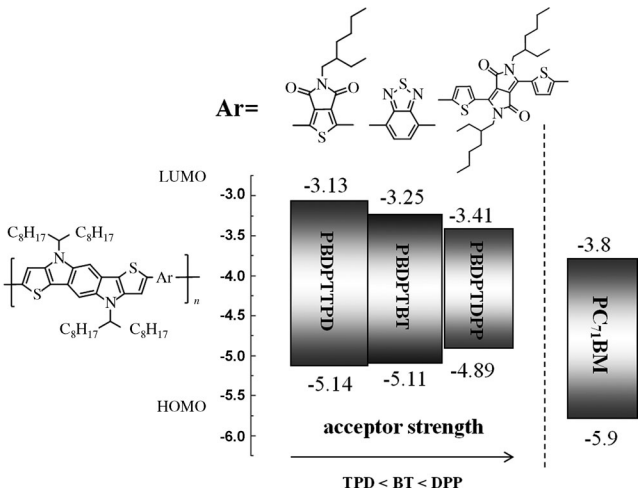


Figure 4. HOMO and LUMO energy levels of the polymers estimated by CV.

  

HOMO energy levels are estimated to be −5.14, −5.11, and −4.89 eV for **PBDPTTPD**, **PBDPTBT**, and **PBDPTDPP**, respectively. This variation indicates that the electron-deficient unit is an important factor to determine the HOMO energy levels, and the **TPD**-based polymers generally have a lower-lying HOMO energy level.[12] Again, relative to the HOMO level of carbon-bridged **PIDTBT** at −5.36 eV and silicon-bridged **PBSTTBT** at −5.32 eV, the relatively higher HOMO energy of **PBDPTBT** (−5.11 eV) is consistent with the more electron-rich nature of **BDPT** leading to the higher oxidation potential. The HOMO–LUMO energy diagram of the polymers is shown in Figure 4.

### Organic Field-Effect Transistors (OFETs) and Photovoltaic Characteristics

It is desirable to utilize these polymers for application in organic field-effect transistors in view of the coplanar geometry and rigid structure of **BDPT**. The hole mobilities of solution-processed polymers were measured by using a bottom-gate, top-contact device configuration with evaporated gold source/drain electrodes and octadecyltrichlorosilane-modified $SiO_2$ gate dielectric on an n-doped silicon wafer surface. The output and transfer plots of the devices exhibited typical *p*-channel OFET characteristics (Figure 5). The hole mobilities were obtained from the transfer characteristics of the

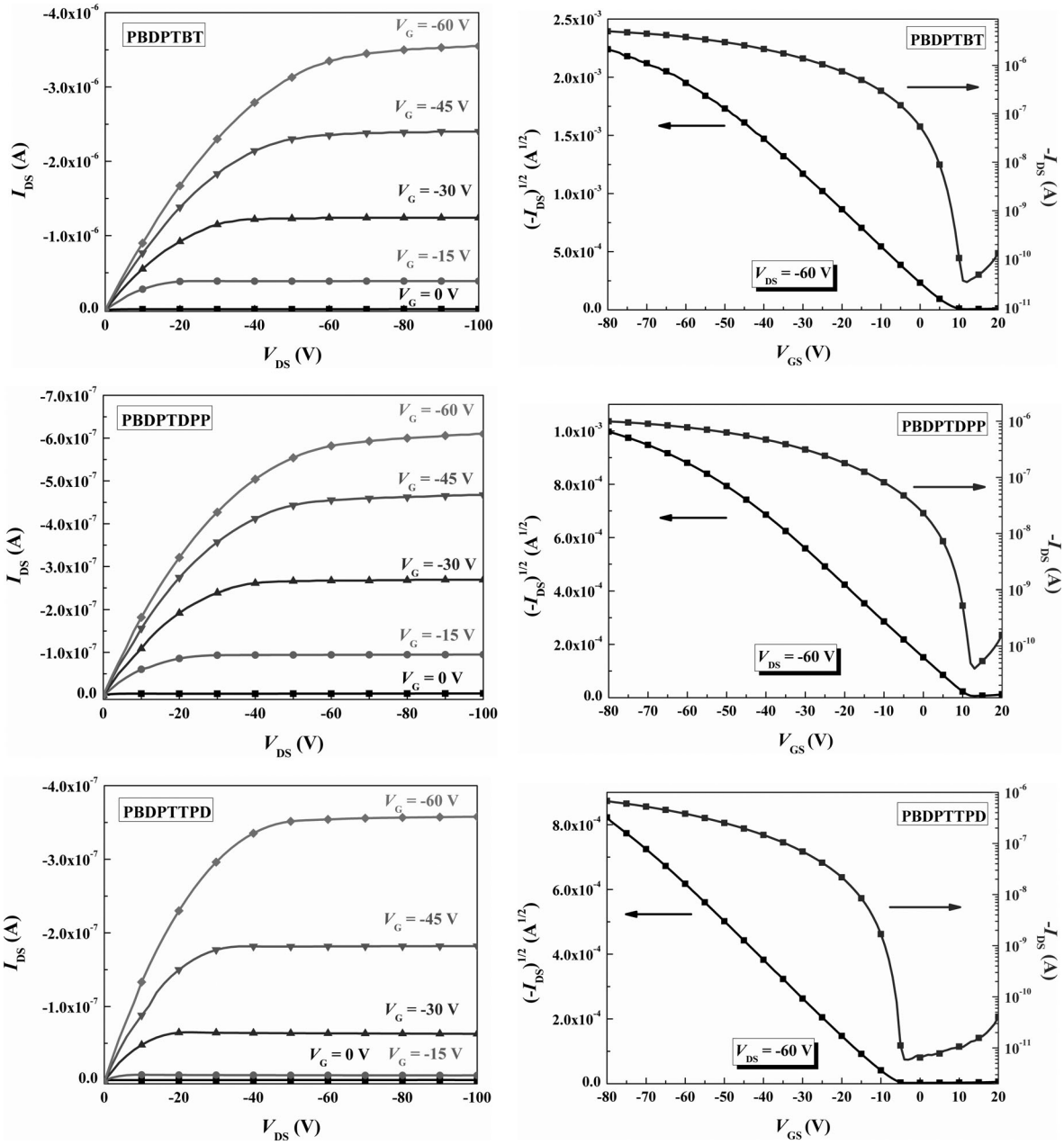


Figure 5. Typical output curves and transfer plots of the OFET devices based on **PBDPTBT** (top), **PBDPTDPP** (middle), and **PBDPTTPD** (bottom).

  

devices in the saturation regime. **PBDPTDPP** and **PBDPTTPD** annealed at 200 and 250 °C for 10 min under nitrogen and showed high hole mobilities of $0.003\ cm^2V^{-1}s^{-1}$ with an on–off ratio of $2.5\times10^4$ and $0.003\ cm^2V^{-1}s^{-1}$ with an on–off ratio of $1.1\times10^5$, respectively (Table 2). More encouragingly, **PBDPTBT** exhibited the highest hole FET mobilities of $0.02\ cm^2V^{-1}s^{-1}$ with a good on–off ratio of $1.5\times10^5$ in the optimal conditions of annealing at 120 °C for 10 min. The thermal treatment is essential for **BDPT**-based polymers to induce stronger intermolecular stacking and thus enhance the hole mobility. Because each **BDPT**-containing polymer has different electron-deficient units (i.e. **BT**, **DPP**, **TPD**), the heating conditions required for achieving optimal morphology are different. However, elucidation of the annealing temperature–device performance relationship is rather complicated. It should be also noted that the FET mobility of **PBDPTBT** is one order higher than that of silicon-bridged **PBDPTBT** with $2.2\times10^{-3}\ cm^2V^{-1}S^{-1}$ reported in the literature.[10a] This result shows that the nitrogen-bridged **BDPT**-containing donor–acceptor polymers are very promising for FET applications. Moreover, the **BDPT** derivatives are suitable to function as superior hole-transporting materials for optoeletronic applications.

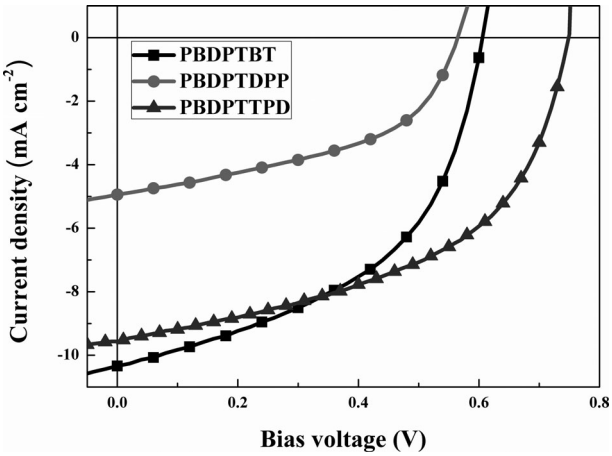


Figure 6. Current density–voltage characteristics of ITO/PEDOT:PSS/polymer:$PC_{71}BM$/Ca/Al devices under illumination of AM 1.5 G at $100\ mW\,cm^{-2}$.

Table 2. Optimized device characteristics.

| Polymer | Blend ratio with $PC_{71}BM$ | $\mu_h$[a] [$cm^2V^{-1}s^{-1}$] | $\mu_h$[b] [$cm^2V^{-1}s^{-1}$] | $V_{oc}$ [V] | $J_{sc}$ [$mA\,cm^{-2}$] | FF [%] | PCE [%] |
|---|---|---|---|---|---|---|---|
| **PBDPTBT** | 1:3 | $5.8\times10^{-5}$ | 0.02 | 0.60 | 10.34 | 49.7 | 3.08 |
| **PBDPTBT**[c] | 1:3 | | | 0.60 | 8.87 | 49 | 2.61 |
| **PBDPTTPD**[d] | 1:3 | $1.1\times10^{-4}$ | 0.003 | 0.75 | 9.69 | 51.2 | 3.72 |
| **PBDPTTPD** | 1:3 | | | 0.74 | 9.3 | 49.04 | 3.37 |
| **PBDPTDPP** | 1:3 | $3.0\times10^{-4}$ | 0.003 | 0.56 | 4.95 | 48.5 | 1.34 |

[a] Hole mobility of polymers determined by space-charge limit current (SCLC). [b] Hole mobility of the polymers determined by OFET. [c] Thermal annealing at 130 °C over 15 min. [d] Thermal annealing at 150 °C over 15 min.

Bulk heterojunction PSCs were fabricated on the basis of a ITO/PEDOT:PSS/polymer:$PC_{71}BM$/Ca/Al configuration and their performances were measured under $100\ mW\,cm^{-2}$ AM 1.5 illumination. Hole-only devices (ITO/PEDOT:PSS/polymer/Au) were also fabricated to estimate the hole mobilities of these polymers through space-charge limit current (SCLC) theory. The characterization data with the optimized fabrication conditions are summarized in Table 2 and the *J*–*V* curves of these devices are shown in Figure 6. The SCLC hole mobility of the polymers follows the trend: **PBDPTDPP** ($3.0\times10^{-4}\ cm^2V^{-1}s^{-1}$) > **PBDPTTPD** ($1.1\times10^{-4}\ cm^2V^{-1}s^{-1}$) > **PBDPTBT** ($5.8\times10^{-5}\ cm^2V^{-1}s^{-1}$). The device using the **PBDPTBT**/$PC_{71}BM$ blend (1:3, w/w) exhibited a $V_{oc}$ of 0.6 V, a $J_{sc}$ of $10.34\ mA\,cm^{-2}$, and a FF of 49.7 %, thus leading to a decent PCE of 3.08 %, whereas the device based on **PBDPTDPP**/$PC_{71}BM$ blend (1:3, w/w) showed a lower $V_{oc}$ of 0.56 V and a $J_{sc}$ of $4.95\ mA\,cm^{-2}$, thereby resulting in a relatively poorer efficiency of 1.34 %. The decreased $V_{oc}$ value of the device is mainly owing to the higher-lying HOMO value of the polymer, and the lower $J_{sc}$ might be attributed to the unfavorable morphology of the active layer. Encouragingly, the device incorporating **PBDPTTPD**/$PC_{71}BM$ (1:3, w/w) composite delivered a high PCE of 3.72 %. This enhanced performance is ascribed to the lower-lying HOMO value of **PBDPTTPD** to yield a higher $V_{oc}$ of 0.75 V. Although **PBDPTTPD** and **PBDPTBT** have similar HOMO energy levels, the **PBDPTTPD** device showed a larger $V_{oc}$ value. The discrepancy may be due to the morphological factor. Donaghey et al. reported two conjugated polymers similar to **PBDPTBT** and **PBDPTTPD** except that they used 2-octyldodecyl side chains in the **BDPT** units and an octyl group in the **TPD** units.[11] However, compared with their reported studies, some improvement and advance in our research should be noted. First, a one-pot amination to synthsize a **BDPT** unit in our case is more straightforward and simpler than the two-step synthesis reported.[11] Second, under similar device fabrication, our devices using **PBDPTBT**/$PC_{71}BM$ (1:3, w/w) and **PBDPTTPD**/$PC_{71}BM$ (1:3, w/w) showed PCEs 3.9 and 3.4 times higher than those reported previously (i.e. 3.08 vs. 0.8 % for **PBDPTBT**-based devices and 3.72 vs. 1.1 % for **PBDPTTPD-**based devices). Such improvement comes from the much higher $J_{sc}$ and $V_{oc}$ values. Relative to the branched and chiral 2-octyldodecyl side chains in the previous reported polymers, **PBDPTBT** and **PBDPTTPD** with shorter and achiral 1-octylnonyl side chains in our research may facilitate molecular assemblies to form better morphologies in the active layers, thereby enhancing the charge-transporting properties. This variation also emphasizes that side-chain engineering of conjugated polymers plays a pivotal role in determining molecular properties and device performance.

  

## Conclusions

In summary, we have synthesized a ladder-type **BDPT** unit in which the two outer thiophene rings are covalently fastened with the central phenylene ring by two nitrogen bridges. The two pyrrole units embedded in **BDPT** were smartly constructed by using one-pot palladium-catalyzed amination. The coplanar **Sn-BDPT** building block was copolymerized with electron-deficient **TPD**, **BT**, and **DPP** acceptors by Stille polymerization. Due to the highly coplanar **BDPT** unit, the **BDPT**-based donor–acceptor copolymers showed strong interchain interactions in the solid state, leading to a significant bathochromic shift and band-broadening of the absorption spectra. Moreover, the electron-donating ability of the nitrogen bridges makes the **BDPT** motif highly electron rich. Therefore, strong photoinduced charge transfer and relatively higher oxidation potential are characteristic of the **BDPT**-based polymers. **PBDPTBT** showed the highest FET hole mobility of $0.02\,cm^2V^{-1}s^{-1}$. The device using the **PBDPTBT**/$PC_{71}BM$ blend (1:3, w/w) exhibited a $V_{oc}$ of 0.6 V, a $J_{sc}$ of $10.34\,mA\,cm^{-2}$, and a FF of 49.7%, thus leading to a decent PCE of 3.08%. Encouragingly, the device incorporating the **PBDPTTPD**/$PC_{71}BM$ (1:3, w/w) composite delivered a high PCE of 3.72%. The enhanced performance is ascribed to the lower-lying HOMO value of **PBDPTTPD** to yield a higher $V_{oc}$ of 0.75 V. This research provides a useful insight into the future molecular design of donor–acceptor copolymers for FET and solar cell applications.

## Experimental Section

*General Measurements and Characterizations*

All chemicals are purchased from Aldrich or Acros and used as received unless otherwise specified. $^1H$ and $^{13}C$ NMR spectra were measured by using a Varian 300 MHz instrument spectrometer. Differential scanning calorimetry (DSC) was measured on a TA Q200 Instrument and thermogravimetric analysis (TGA) was recorded on a Perkin–Elmer Pyris under a nitrogen atmosphere at a heating rate of $10\,°C\,min^{-1}$. Absorption spectra were collected on a HP8453 UV/Vis spectrophotometer. The molecular weights of polymers were measured by the GPC method on a Viscotek VE2001GPC, and polystyrene was used as the standard (THF as the eluent). The electrochemical CV was conducted on a CH Instruments Model 611D. A carbon glass coated with a thin polymer film was used as the working electrode and $Ag/Ag^+$ electrode as the reference electrode, whereas 0.1 M tetrabutylammonium hexafluorophosphate ($Bu_4NPF_6$) in acetonitrile was the electrolyte. CV curves were calibrated by using ferrocence as the standard, the oxidation potential of which is set at −4.8 eV with respect to zero vacuum level. The HOMO energy levels were obtained from the equation $HOMO = -(E_{ox}^{onset} - E_{(ferrocene)}^{onset} + 4.8)\,eV$. The LUMO levels of polymer were obtained from the equation $LUMO = -(E_{red}^{onset} - E_{(ferrocene)}^{onset} + 4.8)\,eV$.

*Fabrication and Characterization of the BHJ Device*

ITO/Glass substrates were ultrasonically cleaned sequentially in detergent, water, acetone, and *iso*-propanol (IPA). The cleaned substrates were covered by a 30 nm thick layer of PEDOT:PSS (Clevios P provided by Stark) by spin coating. After annealing in a glove box at 150 °C for 30 min, the samples were cooled to room temperature. Polymers were dissolved in *o*-dichlorobenzene (ODCB) and $PC_{71}BM$ (purchased from Nano-C) was added. The solution was then heated at 80 °C and stirred overnight at the same temperature. Prior to deposition, the solution was filtered (1 μm filters). The solution of polymer:$PC_{71}BM$ was then spin-coated to form the active layer. The cathode made of calcium (350 nm thick) and aluminum (1000 nm thick) was sequentially evaporated through a shadow mask under high vacuum ($<10^{-6}$ torr). Each sample consists of 4 independent pixels defined by an active area of $0.04\,cm^2$. Finally, the devices were encapsulated and characterized in air.

*Electrical Characterization under Illumination*

The devices were characterized under $100\,mW\,cm^{-2}$ AM 1.5 simulated light measurement (Yamashita Denso solar simulator). Current–voltage (*J*–*V*) characteristics of PSC devices were obtained by a Keithley 2400 SMU. Solar illumination conforming the JIS Class AAA was provided by a SAN-EI 300 W solar simulator equipped with an AM 1.5G filter. The light intensity was calibrated with a Hamamatsu S1336-5BK silicon photodiode. The performances presented here are the average of the 4 pixels of each device.

*OFETs Fabrication and Characterization*

An n-type heavily doped Si wafer with a $SiO_2$ layer of 300 nm and a capacitance of $11\,nF\,cm^{-2}$ was used as the gate electrode and dielectric layer. Thin films (40–60 nm in thickness) of polymers were deposited on octadecyltrichlorosilane (ODTS)-treated $SiO_2$/Si substrates by spin-coating their *o*-dichlorobenzene solutions ($1\,mg\,mL^{-1}$). Then, the thin films were annealed at different temperatures (120, 200 or 250 °C) for 10 min. Gold source and drain contacts (30 nm in thickness) were deposited by vacuum evaporation on the organic layer through a shadow mask, affording a bottom-gate, top-contact device configuration. Electrical measurements of OTFT devices were carried out at room temperature in air by using a 4156C, Agilent Technologies. The field-effect mobility was calculated in the saturation regime by using the equation $I_{DS} = (\mu W C_i / 2L)(V_G - V_T)^2$, in which $I_{DS}$ is the drain-source current, $\mu$ is the field-effect mobility, $W$ is the channel width (500 μm), $L$ is the channel length (50 μm), $Ci$ is the capacitance per unit area of the gate dielectric layer, and $V_G$ is the gate voltage.

*Preparation of Compound **2***

A 2.5 M solution of *n*BuLi in hexane (11.1 mL, 27.7 mmol) was added dropwise to a solution of 2,3-dibromothiophene (**1**) (6.25 g, 25.8 mmol) in dry THF (20 mL) at −78 °C. After stirring at −78 °C for 1 h, the mixture was warmed up to room temperature. The mixture was added to a solution of zinc(II) bromide (5.82 g, 25.8 mmol) in dry THF (15 mL) at −78 °C and then the mixture was stirred at 0 °C for 1 h.

*Synthesis of Compound **4***

A solution of (3-bromothiophen-2-yl) zinc(II) bromide (**2**) (25.8 mmol) was added to a solution of 1,4-dibromo-2,5-diiodobenzene (**3**)[13] (4.50 g, 9.2 mmol) and $[Pd(PPh_3)_4]$ (0.27 g, 0.23 mmol) in dry THF (30 mL) at room temperature. The mixture was refluxed for 3 h. After removal of the solvent under reduced pressure, the residue was extracted with ethyl acetate (50 mL × 3) and water (100 mL). The collected organic layer was dried over $MgSO_4$. After removal of the solvent under reduced pressure, the residue was purified by column chromatography on silica gel (*n*-hexane) to give a white solid product **4** (1.54 g, 30%). $^1H$ NMR ($CDCl_3$, 300 MHz): $\delta = 7.71$ (s, 2H), 7.42 (d, $J = 5.4$ Hz, 2H), 7.09 ppm (d, $J = 5.4$ Hz, 2H); $^{13}C$ NMR (75 MHz, $CDCl_3$): $\delta = 136.6$, 136.1, 135.1, 130.5, 126.9, 123.5, 111.8 ppm.

*Synthesis of Compound **BDPT***

2,2′-(2,5-dibromo-1,4-phenylene)bis(3-bromothiophene) (**4**) (0.75 g, 1.34 mmol), sodium *tert*-butoxide (1.14 g, 11.8 mmol), tris(dibenzylideneacetone) dipalladium (0.25 g, 0.273 mmol), 2,2′-bis(diphenylphosphino)-1,1′-binaphthyl (0.67 g, 1.07 mmol), and **5**[14] (3.76 g, 14.7 mmol) were dissolved in deoxygenated toluene (15 mL). The reaction mixture was refluxed at 125 °C for 21 h and then extracted with diethyl ether (50 mL × 3) and water (50 mL). The collected organic layer was dried over $MgSO_4$. After removal of the solvent under reduced pressure, the residue was purified by column chromatography on silica gel (*n*-hexane) to give

  

a yellow solid **BDPT** (0.3 g, 30%). $^1$H NMR ($CDCl_3$, 300 MHz): $\delta = 7.66$ (s, 2H), 7.32 (d, $J = 5.1$ Hz, 2H), 7.12 (d, $J = 5.1$ Hz, 2H), 4.47 (br, 2H), 2.14 (br, 4H), 1.90 (br, 4H), 1.14–1.25 (m, 48H), 0.78–0.88 ppm (m, 12H); MS (FAB, $C_{48}H_{76}N_2S_2$): $m/z$: calcd: 745.26; found: 745.

*Synthesis of Monomer **Sn-BDPT***

A 2.5 M solution of *n*BuLi in hexane (0.35 mL, 0.88 mmol) was added dropwise to a solution of **BDPT** (0.26 g, 0.34 mmol) in dry THF (10 mL) at −78 °C. After stirring at −78 °C for 1 h, a 1.0 M solution of chlorotrimethylstannane in THF (1.03 mL, 1.03 mmol) was introduced by syringe to the solution. The mixture solution was warmed up to room temperature and stirred for 12 h. The mixture solution was quenched with water and extracted with diethyl ether (50 mL × 3) and water (50 mL). After removal of the solvent under reduced pressure, compound **Sn-BDPT** was obtained as a yellow solid (0.33 g, 92%). $^1$H NMR (300 MHz, [$D_6$]acetone): $\delta = 7.84$ (s, 2H), 7.40 (s, 2H), 4.70 (br, 2H), 2.26 (br, 4H), 1.91 (br, 4H), 1.40–1.13 (m, 48H), 0.78 (t, 6.6 Hz, 12H), 0.43 ppm (s, 18H).

*Synthesis of **PBDPTBT***

**Sn-BDPT** (178.0 mg, 0.17 mmol), **6** (50.1 mg, 0.17 mmol), tris(dibenzylideneacetone) dipalladium (7.8 mg, 0.0085 mmol), tri(2-methylphenyl)-phosphine (20.7 mg, 0.068 mmol), and deoxygenated chlorobenzene (9 mL) were introduced to a 50 mL round-bottomed flask. The mixture was then degassed by bubbling nitrogen for 10 min at room temperature. The round-bottomed flask was placed into the microwave reactor and reacted for 50 min under 270 Watt. The solution was added into methanol dropwise. The precipitate was collected by filtration and washed by Soxhlet extraction with acetone (24 h) and *n*-hexane (24 h) sequentially. The product was re-dissolved in THF. The Si-Thiol (30.0 mg, 0.034 mmol) was added to the above THF solution to remove the residual Pd catalyst. After filtration and removal of the solvent, the polymer was re-dissolved in THF again and added into methanol to re-precipitate. The purified polymer was collected by filtration and dried under vacuum for 1 day to give a black solid (86 mg, 38%, $M_n = 7424$ g mol$^{-1}$, PDI = 1.37). $^1$H NMR (300 MHz, $CDCl_3$): $\delta = 8.43$ (s, 2H), 8.02 (s, 2H), 7.72 (s, 2H), 4.58 (br, 2H), 2.31 (br, 4H), 2.04 (br, 4H), 1.50–1.00 (m, 48H), 0.88 ppm (br, 12H).

*Synthesis of **PBDPTDPP***

**Sn-BDPT** (137.0 mg, 0.13 mmol), **7** (89.6 mg, 0.13 mmol), tris(dibenzylideneacetone) dipalladium (6.0 mg, 0.0065 mmol), tri(2-methylphenyl)-phosphine (16.0 mg, 0.052 mmol), and deoxygenated chlorobenzene (6 mL) were introduced to a 50 mL round-bottomed flask. The mixture was then degassed by bubbling nitrogen for 10 min at room temperature. The round-bottomed flask was placed into the microwave reactor and reacted for 50 min at 270 W. The solution was added into methanol dropwise. The precipitate was collected by filtration and washed by Soxhlet extraction with acetone (24 h) and *n*-hexane (24 h) sequentially. The product was re-dissolved in THF. The Si-Thiol (22 mg, 0.026 mmol) was added to the above THF solution to remove the residual Pd catalyst. After filtration and removal of the solvent, the polymer was re-dissolved in THF again and added into methanol to re-precipitate. The purified polymer was collected by filtration and dried under vacuum for 1 day to give a blackish/green solid (51 mg, 23%, $M_n = 26407$ g mol$^{-1}$, PDI = 3.49); $^1$H NMR (300 MHz, $CDCl_3$): $\delta = 8.99$ (s, 2H), 7.60 (s, 2H), 7.43 (s, 2H), 7.34 (s, 2H), 4.48 (br, 2H), 4.11 (br, 4H), 2.17 (br, 4H), 1.98 (br, 6H), 1.50–090 (m, 70H), 0.81 ppm (br, 18H)

*Synthesis of **PBDPTTPD***

**Sn-BDPT** (166.0 mg, 0.15 mmol), **8** (67.3 mg, 0.15 mmol), tris(dibenzylideneacetone) dipalladium (7.3 mg, 0.0079 mmol), tri(2-methylphenyl)-phosphine (19.3 mg, 0.063 mmol), and deoxygenated chlorobenzene (7 mL) were introduced to a 50 mL round-bottomed flask. The mixture was then degassed by bubbling nitrogen for 10 min at room temperature. The round-bottomed flask was placed into the microwave reactor and reacted for 50 min under 270 W. The solution was added into methanol dropwise. The precipitate was collected by filtration and washed by Soxhlet extraction with acetone (24 h) and *n*-hexane (24 h) sequentially. The product was re-dissolved in THF. The Si-Thiol (27.4 mg, 0.031 mmol) was added to the above THF solution to remove the residual Pd catalyst. After filtration and removal of the solvent, the polymer was re-dissolved in THF again and added into methanol to re-precipitate. The purified polymer was collected by filtration and dried under vacuum for 1 day to give a per se solid (102 mg, 44%, $M_n = 12261$ g mol$^{-1}$, PDI = 1.60); $^1$H NMR (300 MHz, $CDCl_3$): $\delta = 8.27$ (s, 2H), 7.69 (s, 2H), 4.51 (br, 2H), 3.68 (br, 2H), 2.27 (br, 4H), 1.98 (br, 5H), 1.50–0.85 (m, 59H), 0.82 ppm (br, 15H).

## Acknowledgements

We thank the National Science Council and the "ATU Program" of the Ministry of Education, Taiwan, for financial support.

[1] a) A. C. Arias, J. D. MacKenzie, I. McCulloch, J. Rivnay, A. Salleo, *Chem. Rev.* **2010**, *110*, 3; b) G. Yu, J. Gao, J. C. Hummelen, F. Wudl, A. J. Heeger, *Science* **1995**, *270*, 1789; c) S. Günes, H. Neugebauer, N. S. Sariciftci, *Chem. Rev.* **2007**, *107*, 1324; d) B. C. Thompson, J. M. J. Fréchet, *Angew. Chem.* **2008**, *120*, 62; *Angew. Chem. Int. Ed.* **2008**, *47*, 58; e) Y.-J. Cheng, S.-H. Yang, C.-S. Hsu, *Chem. Rev.* **2009**, *109*, 5868; f) J. Chen, Y. Cao, *Acc. Chem. Res.* **2009**, *42*, 1709.

[2] a) J. Roncali, *Chem. Rev.* **1997**, *97*, 173; b) Y. Li, Y. Zou, *Adv. Mater.* **2008**, *20*, 2952.

[3] a) J. Roncali, *Macromol. Rapid Commun.* **2007**, *28*, 1761; b) M. Forster, K. O. Annan, U. Scherf, *Macromolecules* **1999**, *32*, 3159; c) Z. Zhu, D. Waller, R. Gaudiana, M. Morana, D. Mühlbacher, M. Scharber, C. Brabec, *Macromolecules* **2007**, *40*, 1981; d) J. Jacob, S. Sax, T. Piok, E. J. W. List, A. C. Grimsdale, K. Müllen, *J. Am. Chem. Soc.* **2004**, *126*, 6987; e) A. K. Mishra, M. Graf, F. Grasse, J. Jacob, E. J. W. List, K. Müllen, *Chem. Mater.* **2006**, *18*, 2879; f) M. B. Goldfinger, T. M. Swager, *J. Am. Chem. Soc.* **1994**, *116*, 7895; g) U. Scherf, *J. Mater. Chem.* **1999**, *9*, 1853; h) S. A. Patil, U. Scherf, A. Kadashchuk, *Adv. Funct. Mater.* **2003**, *13*, 609; i) Y. Yao, J. M. Tour, *Macromolecules* **1999**, *32*, 2455.

[4] a) J. L. Brédas, J. P. Calbert, D. A. da Silva Filho, J. Cornil, *Proc. Natl. Acad. Sci. USA* **2002**, *99*, 5804; b) S. Ando, J.-I. Nishida, H. Tada, Y. Inoue, S. Tokito, Y. Yamashita, *J. Am. Chem. Soc.* **2005**, *127*, 5336; c) N.-S. Baek, S. K. Hau, H.-L. Yip, O. Acton, K.-S. Chen, A. K.-Y. Jen, *Chem. Mater.* **2008**, *20*, 5734; d) Y. Liang, Y. Wu, D. Feng, S.-T. Tsai, H.-J. Son, G. Li, L. Yu, *J. Am. Chem. Soc.* **2009**, *131*, 56; e) S. Shinamura, I. Osaka, E. Miyazaki, A. Nakao, M. Yamagishi, J. Takeya, K. Takimiya, *J. Am. Chem. Soc.* **2011**, *133*, 5024.

[5] a) I. Osaka, T. Abe, S. Shinamura, E. Miyazaki, K. Takimiya, *J. Am. Chem. Soc.* **2010**, *132*, 5000; b) I. Osaka, T. Abe, S. Shinamura, K. Takimiya, *J. Am. Chem. Soc.* **2011**, *133*, 6852; c) K. Takimiya, S. Shinamura, I. Osaka, E. Miyazaki, *Adv. Mater.* **2011**, *23*, 4347; d) M. Zhang, Y. Sun, X. Guo, C. Cui, Y. He, Y. Li, *Macromolecules* **2011**, *44*, 7625.

[6] a) H.-Y. Chen, J. Hou, S. Zhang, Y. Liang, G. Yang, Y. Yang, L. Yu, Y. Wu, G. Li, *Nat. Photonics* **2009**, *3*, 649; b) H. Zhou, L. Yang, A. C. Stuart, S. C. Price, S. Liu, W. You, *Angew. Chem.* **2011**, *123*, 3051; *Angew. Chem. Int. Ed.* **2011**, *50*, 2995; c) L. Huo, S. Zhang, X. Guo, F. Xu, F. Li, J. Hou, *Angew. Chem.* **2011**, *123*, 9871; *Angew. Chem. Int. Ed.* **2011**, *50*, 9697; d) S. C. Price, A. C. Stuart, L. Yang, H. Zhou, W. You, *J. Am. Chem. Soc.* **2011**, *133*, 4625; e) Z. He, C. Zhong, X. Huang, W.-Y. Wong, H. Wu, L. Chen, S. Su, Y. Cao, *Adv. Mater.* **2011**, *23*, 4636.

[7] a) Y.-J. Cheng, J.-S. Wu, P.-I. Shih, C.-Y. Chang, P.-C. Jwo, W.-S. Kao, C.-S. Hsu, *Chem. Mater.* **2011**, *23*, 2361; b) C.-H. Chen, Y.-J. Cheng, M. Dubosc, C.-H. Hsieh, C.-C. Chu, C.-S. Hsu, *Chem. Asian J.* **2010**, *5*, 2483; c) C.-H. Chen, C.-H. Hsieh, M. Dubosc, Y.-J. Cheng, C.-S. Hsu, *Macromolecules* **2010**, *43*, 697; d) N. Blouin, A. Michaud, M. Leclerc, *Adv. Mater.* **2007**, *19*, 2295; e) N. Blouin, A. Michaud, D. Gendron, S. Wakim, E. Blair, R. Neagu-Plesu, M. Belletête, G. Durocher, Y. Tao, M. Leclerc, *J. Am. Chem. Soc.* **2008**,

  

*130*, 732; f) J.-S. Wu, Y.-J. Cheng, M. Dubosc, C.-H. Hsieh, C.-Y. Chang, C.-S. Hsu, *Chem. Commun.* **2010**, *46*, 3259; g) Y.-J. Cheng, C.-H. Chen, Y.-S. Lin, C.-Y. Chang, C.-S. Hsu, *Chem. Mater.* **2011**, *23*, 5068; h) C.-H. Chen, Y.-J. Cheng, C.-Y. Chang, C.-S. Hsu, *Macromolecules* **2011**, *44*, 8415.

[8] K.-T. Wong, T.-C. Chao, L.-C. Chi, Y.-Y. Chu, A. Balaiah, S.-F. Chiu, Y.-H. Liu, Y. Wang, *Org. Lett.* **2006**, *8*, 5033.

[9] a) C.-P. Chen, S.-H. Chan, T.-C. Chao, C. Ting, B.-T. Ko, *J. Am. Chem. Soc.* **2008**, *130*, 12828; b) Y. Zhang, J. Zou, H.-L. Yip, K.-S. Chen, D. F. Zeigler, Y. Sun, A. K.-Y. Jen, *Chem. Mater.* **2011**, *23*, 2289; c) M. Zhang, X. Guo, X. Wang, H. Wang, Y. Li, *Chem. Mater.* **2011**, *23*, 4264; d) Y. Zhang, J. Zou, H.-L. Yip, K.-S. Chen, J. A. Davies, Y. Sun, A. K.-Y. Jen, *Macromolecules* **2011**, *44*, 4752; e) W. Zhang, J. Smith, S. E. Watkins, R. Gysel, M. McGehee, A. Salleo, J. Kirkpatrick, S. Ashraf, T. Anthopoulos, M. Heeney, I. McCulloch, *J. Am. Chem. Soc.* **2010**, *132*, 11437; f) Y.-C. Chen, C.-Y. Yu, Y.-L. Fan, L.-I. Hung, C.-P. Chen, C. Ting, *Chem. Commun.* **2010**, *46*, 6503.

[10] a) J.-Y. Wang, S. K. Hau, H.-L. Yip, J. A. Davies, K.-S. Chen, Y. Zhang, Y. Sun, A. K.-Y. Jen, *Chem. Mater.* **2011**, *23*, 765; b) R. S. Ashraf, Z. Chen, D. S. Leem, H. Bronstein, W. Zhang, B. Schroeder, Y. Geerts, J. Smith, S. Watkins, T. D. Anthopoulos, H. Sirringhaus, J. C. de Mello, M. Heeney, I. McCulloch, *Chem. Mater.* **2011**, *23*, 768.

[11] J. E. Donaghey, R. S. Ashraf, Y. Kim, Z. G. Huang, C. B. Nielsen, W. Zhang, B. Schroeder, C. R. G. Grenier, C. T. Brown, P. D′angelo, J. Smith, S. Watkins, K. Song, T. D. Anthopoulos, J. R. Durrant, C. K. Williams, I. McCulloch, *J. Mater. Chem.* **2011**, *21*, 18744.

[12] a) Y. Zou, A. Najari, P. Berrouard, S. Beaupré, B. R. Aïch, Y. Tao, M. Leclerc, *J. Am. Chem. Soc.* **2010**, *132*, 5330; b) C. Piliego, T. W. Holcombe, J. D. Douglas, C. H. Woo, P. M. Beaujuge, J. M. J. Fréchet, *J. Am. Chem. Soc.* **2010**, *132*, 7595; c) T.-Y. Chu, J. Lu, S. Beaupré, Y. Zhang, J.-R. Pouliot, S. Wakim, J. Zhou, M. Leclerc, Z. Li, J. Ding, Y. Tao, *J. Am. Chem. Soc.* **2011**, *133*, 4250; d) C. M. Amb, S. Chen, K. R. Graham, J. Subbiah, C. E. Small, F. So, J. R. Reynolds, *J. Am. Chem. Soc.* **2011**, *133*, 10062.

[13] H. Hart, K. Harada, C. J. F. Du, *J. Org. Chem.* **1985**, *50*, 3104.

[14] W. Yue, Y. Zhao, S. Shao, H. Tian, Z. Xie, Y. Geng, F. Wang, *J. Mater. Chem.* **2009**, *19*, 2199.

Received: February 27, 2012
Revised: April 3, 2012
Published online: June 14, 2012

  